Analytical Biochemistry 419 (2011) 61–66

Contents lists available at SciVerse ScienceDirect

Analytical Biochemistry

journal homepage: www.elsevier.com/locate/yabio

A high-throughput screen for directed evolution of aminocoumarin amide synthetases

Niranjan Parajuli, Gavin J. Williams *

Department of Chemistry, North Carolina State University, Raleigh, NC 27695, USA

ARTICLE INFO

Article history:
Received 11 June 2011
Received in revised form 25 July 2011
Accepted 31 July 2011
Available online 6 August 2011

Keywords:
Directed evolution
Aminocoumarin
High-throughput screening
Natural products

ABSTRACT

The biosynthesis of aminocoumarin antibiotics involves the action of amide synthetases which construct amide bonds between aminocoumarins and various acyl moieties. Libraries of aminocoumarin analogues have been generated by *in vivo* fermentation, via feeding known amide synthetase substrates into producing microbial strains. Critically, such feeding studies rely on the inherent or engineered substrate promiscuity of each amide synthetase. We have initiated a program of directed evolution in order to create mutant amide synthetases for the synthesis of new nonnatural amino coumarin analogues. We used the clorobiocin enzyme CloL as a model amide synthetase to design and validate a fluorimetric high-throughput screen, which can be used to report the activity of mutant amide synthetases toward a broad range of coumarin and acyl donor substrates. Our assay monitors the decrease in fluorescence of aminocoumarins on acylation. The utility of the assay was illustrated by screening a library of amide synthetase mutants created by error-prone PCR. The substrate specificity of an amide synthetase was also rapidly probed using this assay, affording several newly identified substrates. It is anticipated that this high-throughput screen will accelerate the creation of amide synthetase mutants with new specificities by directed evolution.

The biosynthesis of many antibiotics involves the activation of acyl moieties via acyladenylate formation [1]. For example, the aminocoumarins are potent inhibitors of bacterial gyrase, and involve the use of an acyladenylate forming enzyme to construct an amide bond linking an aminocoumarin to various acyl moieties [2]. To date, such amide synthetases have been characterized from the clorobiocin (**1**), novobiocin (**2**), simocyclinone (**3**), coumermycin A_1 (**4**), and rubradirin (**5**) gene clusters, and designated as CloL [3], NovL [4], SimL [5,6], CouL [7,8], and RubC1 [9], respectively (Fig. 1). As a representative example, clorobiocin **1** consists of a 3-amino-4,7-dihydroxycoumarin moiety (ring B) flanked on one side by L-noviose (ring C) and on the other side by a 3-dimethylallyl-4-hydroxybenzoyl moiety (ring A) (Fig. 1). CloL is the aminocoumarin amide synthetase which catalyzes amide bond formation between the prenylated hydroxybenzoyl moiety and the aminocoumarin [3]. The aminocoumarin, deoxysugar, and acyl moiety all contribute to the biological activity of clorobiocin [10–13]. Yet, while aminocoumarins such as clorobiocin show excellent antibacterial activity against gram-positive pathogens [14–16], including methicillin-resistant strains, they display poor toxicity and solubility, and also show low activity against gram-negative bacteria [13]. Accordingly, in the search for analogues that overcome these limitations, the unique substrate specificity of several aminocoumarin amide synthetases has been used for the chemo-enzymatic generation of new aminocoumarin antibiotics [17–19]. For example, the substrate specificity of CloL, NovL, and CouL was tested *in vitro* using a panel of ring A analogues and while CloL proved the most promiscuous of the three synthetases, only around half of ring A analogues tested were efficient (>10% relative activity) substrates for the wild-type CloL synthetase [3]. Moreover, by feeding ring A analogues to aminocoumarin producing strains defective in ring A production, milligram scale quantities of novel aminocoumarins could be produced. Notably, *in vivo* analogue yield correlated with *in vitro* aminocoumarin ligase activity.

We therefore reasoned that mutant aminocoumarin amide synthetases with improved activity toward ring A analogues would provide useful catalysts for the *in vivo* production of novel aminocoumarin analogues. Rational engineering of aminocoumarin synthetases is difficult given the lack of any structural information for these enzymes. Accordingly, we turned to directed evolution [20,21] in an effort to discover improved aminocoumarin synthetases. Critically, evolutionary-based enzyme engineering strategies depend on the ability to identify rare improved enzyme variants from large libraries of random mutants, by screening or selection. To date, methods for reporting the activity of aminocoumarin amide synthetases in a high-throughput manner have yet to be reported.

* Corresponding author.
E-mail address: gavin_williams@ncsu.edu (G.J. Williams).

0003-2697/$ - see front matter © 2011 Elsevier Inc. All rights reserved.
doi:10.1016/j.ab.2011.07.037

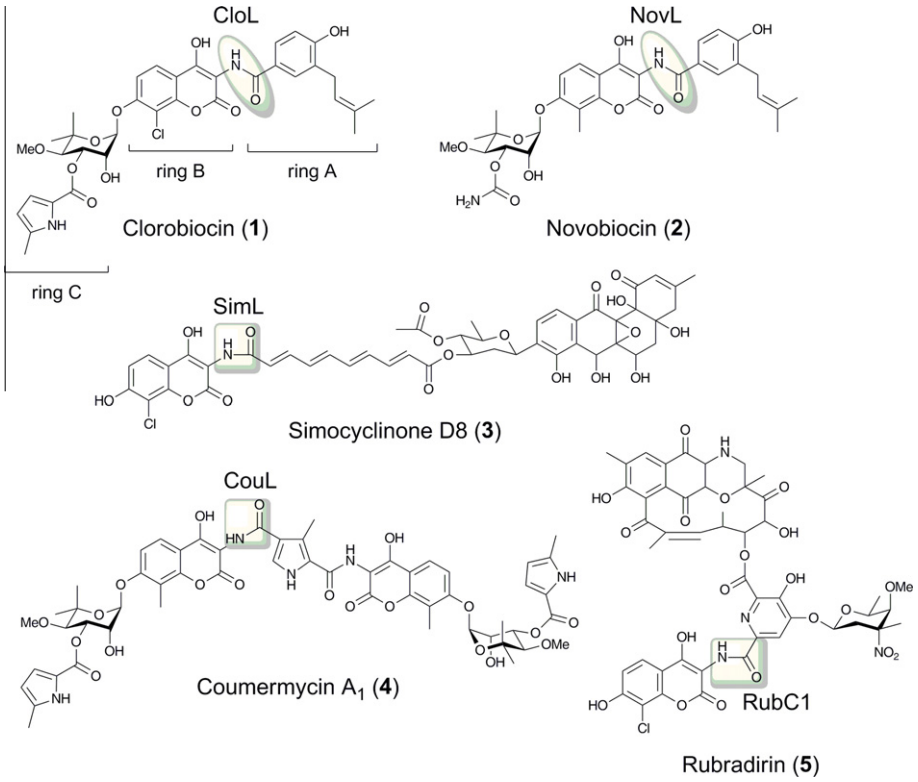

Fig.1. Structure of aminocoumarin antibiotics. The gray boxes highlight the amide bond constructed by the respective amide synthetase; the names of each synthetase are also indicated.

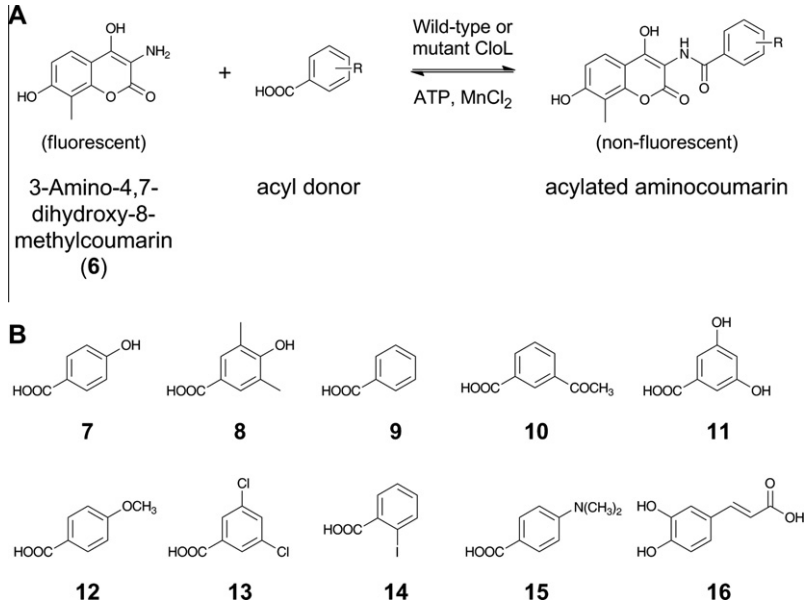

Fig.2. Fluorescence-based assay and the cloL reaction. (A) Strategy for high-throughput screening of the activity of ClolL toward ring A analogues. (B) Structures of ring A analogues used in this study.

Here, we describe the development and validation of a high-throughput screen (HTS)[1] that can be used to identify mutant aminocoumarin synthetases with improved activity toward ring A analogues. This assay is based on the fluorescence properties of aminocoumarins. On acylation by an aminocoumarin synthetase, we expected aminocoumarin fluorescence to decrease sufficiently to allow quantification of enzyme activity by fluorescence spectroscopy (Fig. 2A). ClolL was chosen as a model synthetase to develop and validate the HTS. Although the genuine ClolL aminocoumarin substrate is available via purification from a clorobiocin-producing deletion strain, the synthetase also utilizes the ring B analogue **6** (Fig. 2B), which is available commercially [3]. Thus, aminocoumarin

[1] *Abbreviations used:* HTS, high-throughput screen; IPTG, isopropyl β-D-thiogalactoside, PCR, polymerase chain reaction.

and a panel of acyl donors are available for screening the activity of CloL in sufficient quantity to allow screening large libraries of random mutants produced by error-prone PCR.

Materials and methods

Bacterial strains, plasmid, and chemicals

Reagents were of the highest grade possible and purchased from Sigma (St. Louis, MO). Acyl substrates were purchased either from Sigma (St. Louis, MO) or from Alfa Aesar (Massachusetts, MI). Coumarin **6** was kindly provided by Pfizer (USA). Bacterial strain *Escherichia coli* BL21(DE3)-competent cells were from Promega (Madison, WI). Primers were ordered from Integrated DNA Technologies (Coralville, IA). Analytical HPLC was performed on a Varian ProStar system. Mass spectra were obtained using electrospray ionization on a Thermo TSQ Quantum Discovery MAX connected to a UV/Vis diode array detector. For LC–MS analysis, 1-μl reaction mixtures (quenched with an equal volume of MeOH and diluted 4-fold in H_2O) were analyzed by analytical reverse-phase HPLC with a 2.1 × 50 mm Zorbax SB-C18 5-μm column (Agilent, Santa Clara, CA). A series of linear gradients was developed from 0.1% formic acid/H_2O (A) and 0.1% formic acid/MeOH (B) using the following protocol: 0–5 min, 40% A; 5–6 min, 80% A; 6–6.1 min, 40% A. The flow rate was 250 μl/min, with detection at 305 nm. The MS instrument was operated in positive-ion mode with a capillary voltage of 4 kV, nebulizer pressure of 30 psig, and a drying gas flow rate of 12 L/min at 350 °C.

Construction of recombinant plasmid

Codon optimized *cloL* was synthesized by GenScript (NJ, USA) and provided cloned into a pUC vector via *Nde*I/*Hin*dIII sites. The *cloL* gene from pUC-CloL was amplified using the oligonucleotides CloL-F (5′-CGGCATATGGCGAACAAAGATCATGGCCCGGAAC-3′) and CloL-R (5′-CGGAAGCTTGCGATCCACCAGAACATCCGG-3′) and subcloned into pET22b using the *Nde*I and *Hin*dIII sites (underlined) to afford the vector pET22-CloL.

Mutant library construction

The random mutant library was constructed through error-prone PCR using the Stratagene GeneMorph II Random Mutagenesis Kit, as described by the manufacturer. The PCR was carried out in a 50-μl reaction mixture consisting of 2.5 ng each T7 For (5′-TAATACGACTCACTAATGGG-3′) and T7 Rev (5′-GCTAGTTATTGCTCAGCGG-3′), 0.5 μg of plasmid pET22-CloL, 0.2 mM each dNTP, and 2.5 units of Mutazyme II polymerase in the reaction buffer supplied by the manufacturer. Amplification involved an initial denaturation step at 95 °C for 5 min followed by cycling at 95 °C for 1 min, 60 °C for 1 min, and 72 °C for 1 min for 22 cycles, and then a final extension for 10 min at 72 °C. The *cloL* gene was amplified using oligonucleotides (CloL-F and CloL-R) using 500 ng of pET22-CloL. Amplified product was digested with *Nde*I and *Hin*dIII, purified by agarose gel electrophoresis (0.8% w/v agarose), extracted using the QIAquick Gel Extraction Kit (QIAgen, Valenica, CA), and ligated into similarly treated pET22b. The ligation mixture was transformed into chemically competent NovaBlue cells. Transformants were randomly selected for isolation of plasmid DNA and insertion of mutated-*cloL* was confirmed by restriction enzyme analysis, followed by DNA sequencing. Subsequently, all the transformants from this library were pooled and cultured overnight in LB media containing 100 μg/ml ampicillin. Plasmid was prepared from this culture and used to transform chemical competent *E. coli* BL21(DE3), which were screened as described below.

Expression and purification of CloL

E. coli BL21 (DE3) harboring pET22-CloL was cultured in 10 ml LB medium containing 10 μg/ml ampicillin. Overnight-cultured cells were transferred into 500 ml fresh LB medium supplemented with 500 μg/ml ampicillin, and cells were allowed to grow at 37 °C to an optical density of ~0.6 at 600 nm. The culture was induced with 0.5 mM isopropyl β-D-thiogalactoside (IPTG), and was incubated at 20 °C for 20 h. *E. coli* cells were harvested by centrifugation and washed twice with cold 50 mM sodium phosphate buffer (pH 7.4) containing 300 mM NaCl and 10% (v/v) glycerol. The cells were disrupted ultrasonically, and then centrifuged for 30 min. Finally, the soluble faction was loaded onto a 1 ml HisTrap HP column (GE Healthcare, Piscataway, NJ) and purified by FPLC using the following buffers: wash buffer [50 mM sodium phosphate buffer (pH 7.4) containing 300 mM NaCl and 20 mM imidazole] and elution buffer [50 mM sodium phosphate buffer (pH 7.5) containing 300 mM NaCl and 200 mM imidazole]. The purified protein was concentrated using an Amicon Ultra 30,000 MW centrifugal filter (Millipore Corp., Billerica, MA) and stored as 10% (v/v) glycerol stocks in 50 mM Tris/HCl, pH 8.0, at −80 °C. Protein purity was verified by SDS–PAGE. Protein quantification was carried out using the Bradford Protein Assay Kit from Bio-Rad.

HPLC-based enzyme assay

The amide synthetase assay mixture contained 0.25 mM **6**, 1 mM acyl donor (**7**–**16**), 0.5 mM ATP, 5 mM $MnCl_2$, 50 mM Tris/HCl, pH 8.0, and 25 μl crude cell-free extracts (or purified protein, typically 1–5 μg) in a total volume of 100 μl. Incubation was carried out at 30 °C for 20 min. The reaction was stopped by addition of 100 μl ice-cold methanol, centrifuged at 10,000*g* for 10 min, and 15 μl cleared supernatants used for HPLC analysis. The flow rate was 1 ml/min, and the absorbance was monitored at 305 nm using a Pursuit XRs C18 column (250 × 4.6 mm, Varian Inc.) with a gradient of 100% MeOH and 1% aqueous formic acid and detection at 305 nm. A series of linear gradients was developed from 0.1% formic acid/H_2O (A) and MeOH (B) using the following protocol: 0–10 min, 100% A; 10–21 min, 30% A; 21–30 min, 10% A; 30–35 min, 5% A.

Expression of CloL in 96-deep-well microtiter plate

An Eppendorf epMotion liquid handling machine (Hauppauge, NY) was used for liquid transfer steps. Individual colonies of *E. coli* BL21(DE3)/pET22b-CloL or *E. coli* BL21(DE3)/pET22b were used to inoculate wells of a round-bottomed 96-deep-well plate (VWR) containing 1 ml LB medium supplemented with 100 μg/ml ampicillin. Culture plates were tightly sealed with AeraSeal breathable film (Research Products International Corp.) and incubated at 37 °C and 350 rpm for 18 h. One hundred microliters of each culture was transformed to a freshly prepared deep-well plate containing 1 ml of LB medium supplemented with 100 μg/ml ampicillin. The freshly inoculated plate was incubated at 37 °C and 350 rpm for 3.5 h, at which point protein expression was induced with 0.5 mM IPTG. The plate was incubated for 20 h at 20 °C and 350 rpm. Cells were harvested by centrifugation at 4500*g* for 20 min and resuspended in 100 μl of 50 mM Tris/HCl, pH 8.0, containing 10% glycerol and 10 mg/ml of lysozyme. The plates were then subjected to a single cycle of freeze/thaw, the cell debris was collected by centrifugation at 4500*g* for 20 min, and 25 μl of each cleared extract was used for enzyme assay.

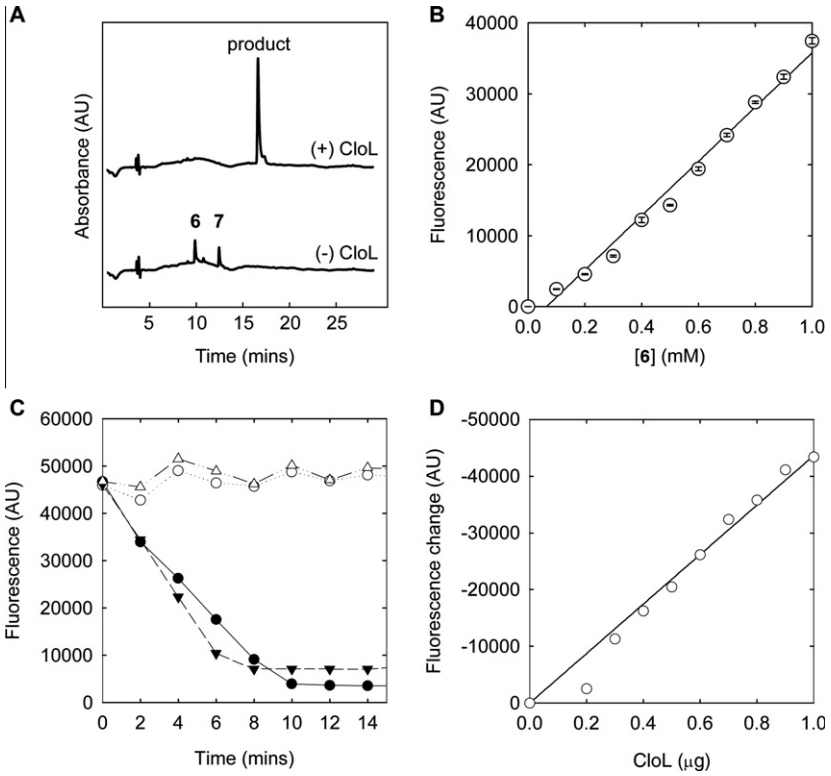

Fig.3. Assay range and cloL characterization. (A) HPLC chromatograms showing cloL-dependent production of a new product peak. (B) Linear fluorescence detection range of **6** in microtiter plate. Each data point represents the average of three measurements; error bars indicate the standard deviation. (C) Fluorescence time course showing CloL-dependent consumption of **6**. Purified CloL (●); no enzyme (○); pET22b-CloL crude extract (▼); pET22b crude extract (▽). (D) Linear detection range of the end-point fluorescence assay using different amounts of purified CloL. For C and D, standard deviations were less than 15% the mean.

General fluorescence assay

For the end-point assay, each assay contained 0.25 mM **6**, 0.5 mM ATP, 5 mM $MnCl_2$, and 50 mM Tris/HCl, pH 8.0, in a total volume of 100 μl. Reaction mixtures also contained CloL (5 μg in pure format or 50 μg total protein in crude extract format) and 1 mM acyl donor **7**. On mixing, the initial fluorescence (λ_{ex} = 355 nm, λ_{em} = 460 nm) was measured using a BioTek Hybrid Synergy 4 plate reader (Winooski, VT) and aliquots were removed at timely intervals (e.g., 0–15 min) for fluorescence assay.

Substrate specificity

Reaction conditions were as described above, except that 25 μl of cleared extract and 1 mM acyl donor (**7**–**16**) were used, and aliquots were taken for fluorescence reading at 0 and 20 min.

High-throughput fluorescence screening assay

For the high-throughput screening reaction, each assay contained 25 μl of cleared extract, 0.25 mM **6**, 1 mM acyl donor (**7**–**16**), 0.5 mM ATP, 5 mM $MnCl_2$, and 50 mM Tris/HCl, pH 8.0, in a total volume of 100 μl. On mixing, the initial fluorescence (λ_{ex} = 355 nm, λ_{em} = 460 nm) was measured using a BioTek Hybrid Synergy 4 plate reader and incubated for 20 min and the fluorescence measurements were repeated.

Results and discussion

We chose CloL as a model aminocoumarin amide synthetase to develop our high-throughput screen and ultimately test our directed evolution strategy. The *clol* gene [3] was cloned into pET22b as a C-terminal His_6-tagged fusion protein, affording the plasmid pET22b-CloL. As expected, subsequent overexpression in *E. coli* BL21 (DE3) and purification by nickel-affinity chromatography afforded the soluble protein in good yield [3]. In order to confirm the enzymatic activity of CloL, we used the ring B analogue **6**, as acyl acceptor, and the ring A analogue 4-hydroxybenzoic acid (**7**, Fig. 2B) as acyl donor, both of which are good substrates for wild-type (WT) CloL [3]. Incubation of CloL with coumarin **6**, acyl component **7**, and ATP resulted in the production of a new product peak, as detected by HPLC (Fig. 3A). Identity of this new peak as the expected amide product was confirmed by LC–MS (Table 1).

With confirmation that the previously established activity of CloL could be reconstituted *in vitro*, we next turned our attention to validating our proposed HTS. The earlier observation that novobiocic acid is nonfluorescent [22] led us to speculate that other aminocoumarins are also nonfluorescent (e.g., **1**, **3**–**5**, Fig. 1), while the nonacylated aminocoumarin acceptors, such as the ring B analogue **6**, would be fluorescent. Thus, we expected that the activity of CloL could be reported by monitoring the decrease in aminocoumarin fluorescence on enzyme-catalyzed acylation. Indeed, the coumarin **6** was found to be strongly fluorescent with an excitation and emission maximum at 355 and 466 nm, respectively (data not shown). A calibration curve using **6** in buffer established a linear detection range up to 1 mM coumarin, and as little as 0.1 mM (10 nmol total) **6** could be detected (Fig. 3B). Significant fluorescence quenching of the fluorophore **6** was observed when exposed more than once to the microplate reader lamp (data not shown) in the absence of enzyme. Although this quenching was very slightly minimized by limiting the plate reader lamp intensity and total number of flashes, we recognized that the fluorescence assay could not be used in a continuous format, and instead is

Table 1
LC/MS analysis of CloL reaction products.

Acyl substrate[a]	Product retention time (min)[b]	MS (*m*/*z*)	
		Calcd	Found
7	16.0	350.0635	$[M+Na]^+$ 350.0636
8	22.0	378.0948	$[M+Na]^+$ 378.0939
9	20.1	334.0686	$[M+Na]^+$ 334.0683
10	17.0	376.0792	$[M+Na]^+$ 376.0784
11	15.6	366.0584	$[M+Na]^+$ 366.0577
12	21.4	364.0792	$[M+Na]^+$ 364.0782

Percentage conversions were determined by HPLC and calculated by dividing the integrated area of the aminocoumarin product by the sum of the integrated area of the product plus the integrated area of the remaining coumarin **6**. See Materials and methods for reaction conditions.

[a] See Fig. 2B for structures. Coumarin **6** was the acceptor. Those acyl substrates that did not result in detectable product are omitted (estimated minimal detection limit of 0.1% conversion from **6**).

[b] See Materials and methods for details of HPLC conditions.

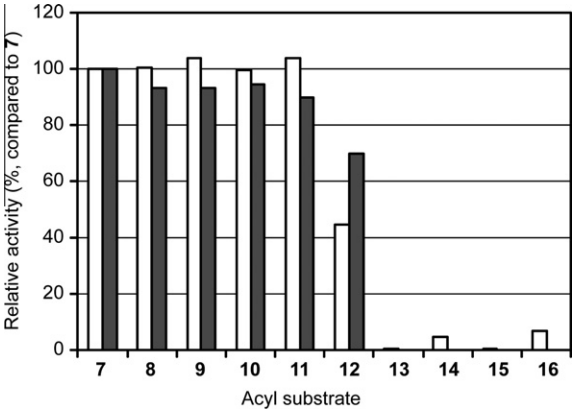

Fig.5. Substrate specificity of cloL in crude extract. Activity of CloL in crude extract with varying acyl components and coumarin **6** was determined using either the fluorescent end-point assay (white bars) or a HPLC-based assay (gray bars). Activity with **7** as substrate was set to 100% using each method. Standard deviations were less than 15% the average.

limited to an end-point design, thereby minimizing exposure of the fluorophore. Accordingly, when CloL was incubated in the presence of **6** and **7**, a significant decrease in fluorescence occurred (Fig. 3C). In contrast, when CloL was absent, no significant change in fluorescence was observed. Moreover, when crude extracts prepared from small scale cultures of *E. coli* BL21 (DE3) that harbored pET22b-CloL or pET22b were used in the assay, significant fluorescence activity was only observed with extract prepared from the CloL overproducing strain (Fig. 3C). Thus, the fluorescence-based assay can report amide synthetase activity even in crude cell extract, and sufficient CloL enzyme is present in a typical crude extract aliquot for fluorimetric detection. In addition, a linear relationship between end-point fluorescence and total enzyme was obtained when between 0.2 and 1.0 μg enzyme was used (Fig. 3D). Cumulatively, these data suggest that aminocoumarin fluorescence is quenched on acylation, and that this provides a strategy for reporting the activity of aminocoumarin amide synthetases.

With proof-of-principle for our fluorescent assay established, we next set out to establish whether it could be used to report the activity of CloL in a high-throughput manner, using crude cell extracts. To establish that this assay was reliable for high-throughput screening in microplate format, we assayed the activity of a total of 96 samples each of positive and negative controls by inoculating colonies of the respective *E. coli* strain into individual wells of a microplate. We used a robotic liquid handling device to carry out all the liquid transfer steps of the cell culturing, crude extract preparation, and assay setup. Fluorimetric assay for acylation of **6** resulted in a standard deviation of ~6% for the extracts containing CloL (Fig. 4A), perfectly adequate for directed evolution experiments. These data demonstrate that CloL activity can be faithfully detected in crude extracts prepared in microtiter plates by our fluorimetric assay.

The fluorimetric assay, in an end-point fashion, was then used to characterize the activities of a small number of CloL variants created by error-prone PCR. Random mutagenesis conditions were adjusted to achieve a mutagenesis rate of 3.5 nucleotides per gene, corresponding to 1–2 amino acid mutations per gene product. The activities of 96 library members are shown in Fig. 4B, displayed in descending order. In contrast to the data presented for the control strains (Fig. 4A), the library contained mutants with a broad range of activities, and as might well be expected, several library members (~50%) did not display any detectable activity with **6** and **7**.

In order to illustrate that our fluorescence assay is suitable for reporting amide synthetase activity toward other acyl components, the substrate specificity of CloL toward a panel of nine ring A analogs (**7**–**16**, Fig. 2B) was probed by a simple end-point fluorescence assay, using CloL present in crude extracts (Fig. 5). In addition, product mixtures were analyzed by HPLC for comparison, and product identities were confirmed by LC–MS analysis (Table 1). Of this small panel, **7**–**9** and **15**–**16** have previously been investigated as substrates [3,23], whereas **10**–**14** have yet to be reported. The standard

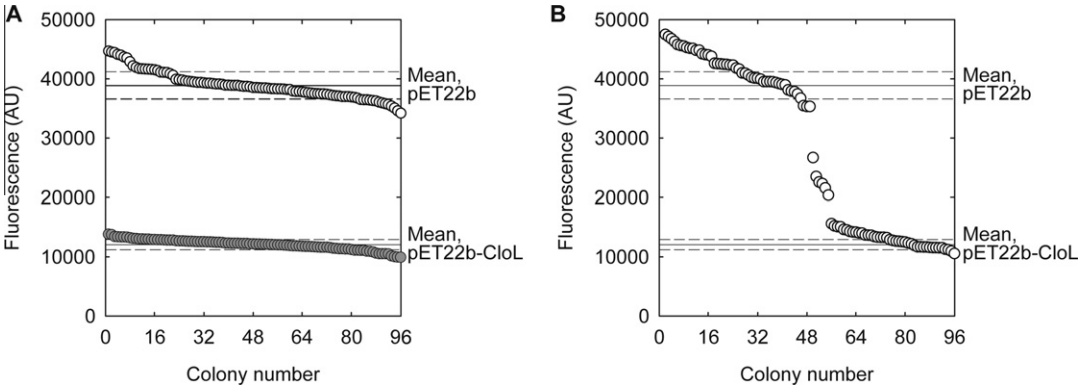

Fig.4. Fluorescence assay in high-throughput format. (A) Activities of pET22b-CloL and pET22b colonies, plotted in descending order. Solid horizontal lines indicate mean activity for pET22b-CloL and pET22b cultures; dashed horizontal lines indicate one standard deviation +/− the mean. (B) Activities of clones from a library of CloL variants produced by error-prone PCR, plotted in descending order. Solid horizontal lines indicate mean activity for pET22b-CloL and pET22b clones; dashed horizontal lines indicate one standard deviation +/− the mean.

deviation for these end-point assays was ~5%; thus successful substrates were those that produced a decrease in fluorescence greater than 5% of the decrease with **7** as substrate. The end-point assay faithfully reported activity toward each acyl component, as compared to that determined by HPLC analysis of the same product mixtures (Fig. 5). For example, **13**–**16** were not detectable substrates (<10% relative activity, compared to **7**) in the fluorescence assay, and product peak could not be detected by HPLC. Yet, **7**–**11** each showed close to 100% activity (compared to **7** as substrate), while *p*-anisic acid **12** displayed ~45% activity, compared to that with **7**. As expected, crude extracts that lack CloL failed to produce significant change in fluorescence, and did not show new product peaks by HPLC (data not shown). These results agree well with the previously reported substrate specificity of CloL [3,23].

Discussion

In this study, we have developed a fluorescent HTS for amide synthetase activity that is convenient, fast, and reliable. To the best of our knowledge, this represents the first HTS available for reporting the activity of natural product amide synthetases. High-throughput screens based on coumarins are well known, including in directed evolution experiments [24–27], but have not previously been applied to amide synthetases. In addition, given that the screen relies simply on the coumarin fluorescence decrease on amide bond formation, the screen can be applied to a broad substrate range of acyl donors, and potentially to other coumarin analogues, without significantly changing the protocol. Moreover, enzyme substrates do not require modification in any way, and therefore resemble closely the structure of the desired final product. Furthermore, this screen should be applicable to other amide synthetases involved in aminocoumarin biosynthesis, including NovL, CouL, and SimL.

Although quenching of the coumarin fluorophore due to exposure to light prevented the screen to be performed as a continuous assay, the screen could still be used to great effect in an end-point format. For example, we were able to rapidly and effectively determine the substrate specificity of CloL. Notably, this analysis led to the identification of three new CloL substrates (**10**–**12**). Further, this information can now be used to guide future substrate specificity engineering efforts. Utility of the fluorescence-based assay was also proved by screening a small portion of library of CloL mutants generated by error-prone PCR. Although (not surprisingly) no improved mutants were identified from this pilot screen, we are currently screening several thousand members of the library using acyl donors **7**–**12**. Additionally, focused random mutagenesis may ultimately prove more efficient. For example, sequence comparison of CouL, NovL, and CloL revealed a ~25 amino acid region that is highly variable and likely represents a specificity conferring region in these and other acyladenylate forming enzymes [8]. Random or semirandom mutagenesis of this region may yield mutant enzymes with altered substrate specificity.

The availability of a high-throughput screening platform for amide synthetases will likely accelerate the creation of mutant enzymes with altered substrate specificities for the synthesis of aminocoumarin analogues. We plan to use engineered amide synthetases as *in vivo* biocatalysts for the fermentation of aminocoumarins in *Streptomyces* strains deficient in ring A production.

References

[1] M.A. Marahiel, L.O. Essen, Nonribosomal peptide synthetases: mechanistic and structural aspects of essential domains, Methods Enzymol. 458 (2009) 337–351.
[2] L. Heide, The aminocoumarins: biosynthesis and biology, Nat. Prod. Rep. 26 (2009) 1241–1250.
[3] U. Galm, M.A. Dessoy, J. Schmidt, L.A. Wessjohann, L. Heide, In vitro and in vivo production of new aminocoumarins by a combined biochemical, genetic, and synthetic approach, Chem. Biol. 11 (2004) 173–183.
[4] M. Steffensky, S.M. Li, L. Heide, Cloning, overexpression, and purification of novobiocic acid synthetase from *Streptomyces spheroides* NCIMB 11891, J. Biol. Chem. 275 (2000) 21754–21760.
[5] M. Pacholec, C.L. Freel Meyers, M. Oberthur, D. Kahne, C.T. Walsh, Characterization of the aminocoumarin ligase SimL from the simocyclinone pathway and tandem incubation with NovM,P,N from the novobiocin pathway, Biochemistry 44 (2005) 4949–4956.
[6] T. Luft, S.M. Li, H. Scheible, B. Kammerer, L. Heide, Overexpression, purification and characterization of SimL, an amide synthetase involved in simocyclinone biosynthesis, Arch. Microbiol. 183 (2005) 277–285.
[7] C.L. Freel Meyers, M. Oberthur, L. Heide, D. Kahne, C.T. Walsh, Assembly of dimeric variants of coumermycins by tandem action of the four biosynthetic enzymes CouL, CouM, CouP, and NovN, Biochemistry 43 (2004) 15022–15036.
[8] E. Schmutz, M. Steffensky, J. Schmidt, A. Porzel, S.M. Li, L. Heide, An unusual amide synthetase (CouL) from the coumermycin A1 biosynthetic gene cluster from *Streptomyces rishiriensis* DSM 40489, Eur. J. Biochem. 270 (2003) 4413–4419.
[9] B. Boll, S. Hennig, C. Xie, J. Kyong Sohng, L. Heide, Adenylate-forming enzymes of rubradirin biosynthesis: RubC1 is a bifunctional enzyme with aminocoumarin acyl ligase and tyrosine-activating domains, ChemBioChem 12 (2011) 1105–1114.
[10] R.J. Lewis, O.M. Singh, C.V. Smith, T. Skarzynski, A. Maxwell, A.J. Wonacott, D.B. Wigley, The nature of inhibition of DNA gyrase by the coumarins and the cyclothialidines revealed by X-ray crystallography, EMBO J. 15 (1996) 1412–1420.
[11] F.T. Tsai, O.M. Singh, T. Skarzynski, A.J. Wonacott, S. Weston, A. Tucker, R.A. Pauptit, A.L. Breeze, J.P. Poyser, R. O'Brien, J.E. Ladbury, D.B. Wigley, The high-resolution crystal structure of a 24-kDa gyrase B fragment from *E. coli* complexed with one of the most potent coumarin inhibitors, clorobiocin, Proteins 28 (1997) 41–52.
[12] D. Lafitte, V. Lamour, P.O. Tsvetkov, A.A. Makarov, M. Klich, P. Deprez, D. Moras, C. Briand, R. Gilli, DNA gyrase interaction with coumarin-based inhibitors: the role of the hydroxybenzoate isopentenyl moiety and the 5′-methyl group of the noviose, Biochemistry 41 (2002) 7217–7223.
[13] A. Maxwell, The interaction between coumarin drugs and DNA gyrase, Mol. Microbiol. 9 (1993) 681–686.
[14] Raad II, R.Y. Hachem, D. Abi-Said, K.V. Rolston, E. Whimbey, A.C. Buzaid, S. Legha, A prospective crossover randomized trial of novobiocin and rifampin prophylaxis for the prevention of intravascular catheter infections in cancer patients treated with interleukin-2, Cancer 82 (1998) 403–411.
[15] I. Raad, R. Darouiche, R. Hachem, M. Sacilowski, G.P. Bodey, Antibiotics and prevention of microbial colonization of catheters, Antimicrob. Agents Chemother. 39 (1995) 2397–2400.
[16] T.J. Walsh, H.C. Standiford, A.C. Reboli, J.F. John, M.E. Mulligan, B.S. Ribner, J.Z. Montgomerie, M.B. Goetz, C.G. Mayhall, D. Rimland, et al., Randomized double-blinded trial of rifampin with either novobiocin or trimethoprim-sulfamethoxazole against methicillin-resistant *Staphylococcus aureus* colonization: prevention of antimicrobial resistance and effect of host factors on outcome, Antimicrob. Agents Chemother. 37 (1993) 1334–1342.
[17] L. Heide, Aminocoumarins mutasynthesis, chemoenzymatic synthesis, and metabolic engineering, Methods Enzymol. 459 (2009) 437–455.
[18] C. Anderle, S. Hennig, B. Kammerer, S.M. Li, L. Wessjohann, B. Gust, L. Heide, Improved mutasynthetic approaches for the production of modified aminocoumarin antibiotics, Chem. Biol. 14 (2007) 955–967.
[19] H. Xu, L. Heide, S.M. Li, New aminocournarin antibiotics formed by a combined mutational and chemoenzymatic approach utilizing the carbamoyltransferase novN, Chem. Biol. 11 (2004) 655–662.
[20] P.A. Romero, F.H. Arnold, Exploring protein fitness landscapes by directed evolution, Nat. Rev. Mol. Cell. Biol. 10 (2009) 866–876.
[21] C.A. Tracewell, F.H. Arnold, Directed enzyme evolution: climbing fitness peaks one amino acid at a time, Curr. Opin. Chem. Biol. 13 (2009) 3–9.
[22] G.J. Williams, R.D. Goff, C. Zhang, J.S. Thorson, Optimizing glycosyltransferase specificity via "hot spot" saturation mutagenesis presents a catalyst for novobiocin glycorandomization, Chem. Biol. 15 (2008) 393–401.
[23] S. Alt, N. Burkard, A. Kulik, S. Grond, L. Heide, An artificial pathway to 3,4-dihydroxybenzoic acid allows generation of new aminocoumarin antibiotic recognized by catechol transporters of *E. coli*, Chem. Biol. 18 (2011) 304–313.
[24] G.J. Williams, J.S. Thorson, A high-throughput fluorescence-based glycosyltransferase screen and its application in directed evolution, Nat. Protocols 3 (2008) 357–362.
[25] G.J. Williams, C. Zhang, J.S. Thorson, Expanding the promiscuity of a natural-product glycosyltransferase by directed evolution, Nat. Chem. Biol. 3 (2007) 657–662.
[26] R.D. Gupta, M. Goldsmith, Y. Ashani, Y. Simo, G. Mullokandov, H. Bar, M. Ben-David, H. Leader, R. Margalit, I. Silman, J.L. Sussman, D.S. Tawfik, Directed evolution of hydrolases for prevention of G-type nerve agent intoxication, Nat. Chem. Biol. 7 (2011) 120–125.
[27] K.E. Griswold, N.S. Aiyappan, B.L. Iverson, G. Georgiou, The evolution of catalytic efficiency and substrate promiscuity in human theta class 1–1 glutathione transferase, J. Mol. Biol. 364 (2006) 400–410.